

Transient solute transport with sorption in Poiseuille flow

Li Zhang^{1,2}, Marc A. Hesse^{2,3†} and Moran Wang¹

¹Department of Engineering Mechanics and CNMM, Tsinghua University, Beijing, 100084, China

²Department of Geological Sciences, University of Texas at Austin, Austin, TX, 78712, US

³Institute of Computational Engineering and Sciences, University of Texas at Austin, Austin, TX, 78712, US

(Received xx; revised xx; accepted xx)

Previous work on solute transport with sorption in Poiseuille flow has reached contradictory conclusions. Some have concluded that sorption increases mean solute transport velocity and decreases dispersion relative to a tracer, while others have concluded the opposite. Here we resolve this contradiction by deriving a series solution for the transient evolution that recovers previous results in the appropriate limits. This solution shows a transition in solute transport behavior from early to late time that is captured by the first- and zeroth-order terms. Mean solute transport velocity is increased at early times and reduced at late times, while solute dispersion is initially reduced, but shows a complex dependence on the partition coefficient k at late times. In the equilibrium sorption model, the time scale of the early regime and the duration of the transition to the late regime both increase with $\ln k$ for large k . The early regime is pronounced in strongly-sorbing systems ($k \gg 1$). The kinetic sorption model shows a similar transition from the early to the late transport regime and recovers the equilibrium results when adsorption and desorption rates are large. As the reaction rates slow down, the duration of the early regime increases, but the changes in transport velocity and dispersion relative to a tracer diminish. In general, if the partition coefficient k is large, the early regime is well-developed and the behavior is well characterized by the analysis of the limiting case without desorption.

Key words:

1. Introduction

Reactive solute transport with surface reaction is common in natural and engineering applications such as solute separation in chromatography (Hlushkou *et al.* 2014), contaminant transport in porous media (Hesse *et al.* 2010) and particle transport in biological systems (Shipley & Waters 2012). Solute transport in a channel with Poiseuille flow and sorbing boundaries provides a simplified model system that allows an understanding of the effect of reactions on the macroscopic transport velocity and dispersion of the solute. This two-dimensional configuration resembles some microfluidic systems used in chromatography and biomaterial delivery and provides insight of solute transport in fractures (Wels *et al.* 1997). In these systems, the macroscopic properties are given

† Email address for correspondence: mhesse@jsg.utexas.edu

by transverse averaging. In the absence of surface reactions, the solute is a tracer and the average transport velocity of the tracer is identical to the mean flow velocity and its dispersion is given by Taylor's analysis (Taylor 1953). However, previous work has reached contradictory conclusions as to the effect of sorption on solute transport velocity and dispersion.

For channel flow with first-order, *irreversible* adsorption reaction, previous analyses have shown that adsorption increases transport velocity and decreases the dispersion of the solute relative to a tracer in the asymptotic regime (Sankarasubramanian & Gill 1973; De Gance & Johns 1978*a,b*; Lungu & Moffatt 1982; Smith 1983; Barton 1984; Shapiro & Brenner 1986; Balakotaiah & Chang 1995; Mikelić *et al.* 2006; Biswas & Sen 2007). The solute velocity increases because adsorption removes solutes from the slow-moving fluid near the wall so that the solute preferentially samples the fast-moving fluid in the center of the channel. This can increase the transport velocity by up to 30% with increasing adsorption in planar Poiseuille flow (Lungu & Moffatt 1982).

However, this is in contrast to the results in chromatography showing that adsorption reduces the transport velocity due to the continuous removal of the solute from the concentration front (Golay 1958; Khan 1962). The chromatographic analysis considers a *reversible* reaction that allows both adsorption and desorption. In this case, the transport of solute is determined by the partition coefficient k , the ratio of adsorbed mass over aqueous mass. Concretely, the transversely-averaged transport velocity will be reduced by a factor of $1/(1+k)$ relative to the mean flow velocity. Similarly, different results have been reached with respect to the effect of adsorption on the dispersion coefficient. Chromatographic analysis shows a complex dependence of dispersion on k while dispersion is reduced in the former case.

The main difference between these two contrasting analyses is that one only considers adsorption (e.g. Lungu & Moffatt 1982) while the other considers both adsorption and desorption (e.g. Khan 1962). One might therefore expect that the reversible analysis recovers the results of the irreversible one in the limit of negligible desorption. However, in this limit the discrepancy between the two analyses is the largest. The transport velocity vanishes in the reversible case while it is finite in the irreversible case. This apparent contradiction may be reconciled by the observation that solute transport undergoes a transition from an early regime characterized by increased solute velocity to a late regime characterized by decreased solute velocity (Paine *et al.* 1983; Balakotaiah & Chang 1995).

Here we present an analysis that demonstrates the transition in solute transport behavior reconciles the reversible and irreversible analyses. To this end, we study solute transport in a two-dimensional straight channel with adsorption onto and desorption from the walls. We use the method of moments in combination with the Laplace transform to derive a set of series solutions for zeroth-, first- and second-order longitudinal moments valid for all times. It is shown that the zeroth-order terms in the series solution corresponds to the late time behavior, while the first-order terms corresponds to the early time behavior. This analysis recovers both the previous results and therefore reconciles them. Moreover, it allows us to quantify the transition for equilibrium and kinetic sorption models. The manuscript is structured as follows: the problem is formulated in §2 and solved in §3, followed by a discussion of the transport regimes in §4.

2. Problem formulation

We model single component solute transport in a two-dimensional straight channel with surface adsorption and desorption, which is illustrated in figure 1. The width of

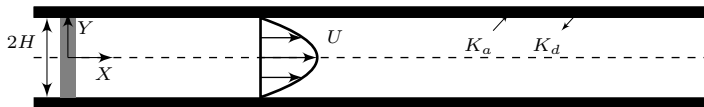


FIGURE 1. In an infinitely long channel, a slender, transversely uniform strip of solute (gray area) is released in the fluid and transported by Poiseuille flow with adsorption and desorption on the walls.

the channel is $2H$ in the Y direction and the length is assumed to be infinite in the X direction. The velocity field is given by an ideal Poiseuille flow, $U(Y) = \frac{3}{2}U_0(1 - Y^2/H^2)$, where U_0 is the mean flow velocity. Adsorption onto and desorption from the walls allow exchange of mass between the solid surface and the fluid.

The mass transport of solute in the fluid is given by the advection–diffusion equation,

$$\frac{\partial C}{\partial T} + U(Y) \frac{\partial C}{\partial X} = D \left(\frac{\partial^2 C}{\partial X^2} + \frac{\partial^2 C}{\partial Y^2} \right), \quad (2.1)$$

where T is the dimensional time [T], C the dimensional solute concentration [ML^{-3}] and D the diffusion coefficient [L^2T^{-1}].

Since the channel is assumed to be infinite, the concentration and any order of its derivative must vanish as $X \rightarrow \pm\infty$. Because of the symmetry along the centerline, $\partial C/\partial Y = 0$, and only the upper half of the domain is considered.

The adsorbed concentration on the wall is assumed to form an infinitely-thin and static surface layer without longitudinal diffusion. The exchange of mass between the wall and the fluid is given as

$$-D \frac{\partial C}{\partial n} = \frac{\partial \Gamma}{\partial T}, \quad (2.2)$$

where n denotes the outward normal direction of the wall and Γ is the dimensional surface concentration [ML^{-2}]. Adsorption and desorption are assumed to be described by the first-order reactions, so that the change of surface concentration is given by

$$\frac{\partial \Gamma}{\partial T} = K_a C - K_d \Gamma, \quad (2.3)$$

where K_a and K_d are the dimensional adsorption and desorption rate constants with dimensions of [LT^{-1}] and [T^{-1}], respectively (Khan 1962). When $K_d = 0$, the linear kinetic model reduces to a first-order, irreversible adsorption reaction. When both K_a and K_d are large, the reaction approaches local chemical equilibrium. At equilibrium, the surface concentration is linearly proportional to solute concentration

$$\Gamma = KC, \quad (2.4)$$

where $K = K_a/K_d$ is the dimensional partition coefficient. Equation (2.4) is also referred to as a linear isotherm (Golay 1958).

Initially, the solute has a uniform transverse distribution at $X = 0$ with no mass adsorbed on the wall and is assumed to be a δ -function in the X direction so that

$$C(X, Y, 0) = \frac{M_I}{A} \delta(X) \quad \text{and} \quad \Gamma(X, 0) = 0, \quad (2.5a,b)$$

where M_I represents the total mass in the system [M] and A is the cross-sectional area of the channel [L^2]. A characteristic concentration is chosen as $C_0 = M_I/(HA)$ to simplify the formulation in dimensionless form. This initial condition, which has been used in previous work, assumes that the system is not in local chemical equilibrium. We note

that the transient solute transport behavior is very sensitive to the initial condition and further analysis of the effect of the initial condition is provided in appendix A.

The following characteristic quantities are chosen to non-dimensionalize the problem,

$$\begin{aligned} x &= X/H, & y &= Y/H, & u &= U/U_0, \\ c &= C/C_0, & \gamma &= \Gamma/(C_0H), & t &= T/(H^2/D). \end{aligned} \quad (2.6)$$

Note that we choose C_0H as characteristic surface concentration and the diffusive time scale H^2/D as the characteristic time scale. Consequently, the dimensionless formulation of the problem is written as

$$\frac{\partial c}{\partial t} + Pe u \frac{\partial c}{\partial x} = \frac{\partial^2 c}{\partial x^2} + \frac{\partial^2 c}{\partial y^2} \quad (2.7a)$$

$$-\frac{\partial c}{\partial y} = \frac{\partial \gamma}{\partial t} \quad \text{at} \quad y = 1, \quad (2.7b)$$

$$\frac{\partial c}{\partial y} = 0 \quad \text{at} \quad y = 0, \quad (2.7c)$$

$$c = \delta(x) \quad \text{at} \quad t = 0, \quad (2.7d)$$

$$\gamma = 0 \quad \text{at} \quad t = 0. \quad (2.7e)$$

If the surface reaction is modelled by the linear kinetic model,

$$\frac{\partial \gamma}{\partial t} = k_a c - k_d \gamma, \quad (2.8)$$

there will be three dimensionless groups in equation (2.7) and (2.8),

$$Pe = \frac{U_0 H}{D}, \quad k_a = \frac{K_a H}{D}, \quad k_d = \frac{K_d H^2}{D}. \quad (2.9)$$

Physically, the Peclet number, Pe , represents the ratio of the transverse diffusive time scale to the longitudinal advective time scale and the Damköhler numbers, k_a and k_d , represent the ratio of the transverse diffusive time scale to the adsorption and desorption time scales, respectively.

Otherwise, if the equilibrium sorption model is used

$$\gamma = kc, \quad (2.10)$$

and the number of dimensionless groups reduces to two by replacing k_a and k_d with

$$k = \frac{k_a}{k_d}. \quad (2.11)$$

In this work, k_a , k_d and k are all assumed to be constants. A value of 10 is chosen for Pe to limit the longitudinal domain size required in numerical simulation. This choice will not affect the key results which are independent of Pe . In the following, we deal with the more general linear kinetic sorption model analytically and results will be given for both the kinetic and equilibrium model in §4.

3. Solution for the longitudinal moments

Following the classical, transverse-averaging idea introduced by Taylor (1953) to reduce the dimension of the problem, we consider the transverse-averaged concentration $\bar{c} = \int_0^1 c dy$ and the distribution of \bar{c} is described by its longitudinal moments $m_n = \int_{-\infty}^{\infty} x^n \bar{c} dx$, where n is the order of the moment. The lower-order moments, e.g. zeroth-,

first- and second-order moments are of most interest to us. Furthermore, we define the normalized longitudinal moments of zeroth-, first- and second-order

$$M_0 = \frac{m_0}{m_I}, \quad M_1 = \frac{m_1}{m_0}, \quad M_2 = \frac{m_2}{m_0} - \left(\frac{m_1}{m_0} \right)^2, \quad (3.1a,b,c)$$

where m_I is the dimensionless initial mass, which is unity here. The fraction of solute in the fluid is given by M_0 . The center of mass and the variance of the solute distribution in the fluid are given by M_1 and M_2 , respectively. Thus, the dimensionless transport velocity and longitudinal dispersion coefficient are

$$v = \frac{dM_1}{dt} \quad \text{and} \quad D_L = \frac{1}{2} \frac{dM_2}{dt}. \quad (3.2a,b)$$

In the following, analytical solutions are derived for lower order moments m_n ($n = 0, 1, 2$) in the form of series solutions.

3.1. Moment equation and solution in the Laplace space

Firstly, following the method of moments developed by Aris (1956), multiply equation (2.7a) by x^n and integrate in the x direction to obtain the equation for $c_n^*(y, t)$,

$$\frac{\partial c_n^*}{\partial t} + Pe u \int_{-\infty}^{\infty} x^n \frac{\partial c}{\partial x} dx = \int_{-\infty}^{\infty} x^n \frac{\partial^2 c}{\partial x^2} dx + \frac{\partial^2 c_n^*}{\partial y^2}, \quad (3.3)$$

where $c_n^* = \int_{-\infty}^{\infty} x^n c dx$ is the n^{th} longitudinal moment of concentration in the filament through y , which is not yet transversely averaged. The moments m_n introduced above are the transverse averages of c_n^* . After integration by parts and noting that the concentration and all of its derivatives vanish at infinity, we have

$$\frac{\partial c_n^*}{\partial t} - nPe u c_{n-1}^* = n(n-1)c_{n-2}^* + \frac{\partial^2 c_n^*}{\partial y^2}, \quad (3.4a)$$

where $c_{-1}^* = c_{-2}^* = 0$. Similarly, the boundary conditions (2.7b) and (2.7c) give

$$-\frac{\partial c_n^*}{\partial y} = \frac{\partial \gamma_n^*}{\partial t} = k_a c_n^* - k_d \gamma_n^* \quad \text{at} \quad y = 1, \quad (3.4b)$$

$$\frac{\partial c_n^*}{\partial y} = 0 \quad \text{at} \quad y = 0, \quad (3.4c)$$

where γ_n^* is defined as the n^{th} longitudinal moment of the surface concentration.

Laplace transform in time reduces (3.4) to a system of ordinary differential equations only involving the transformed variable

$$\hat{c}_n^*(y, s) = \mathcal{L}\{c_n^*\}(s) = \int_0^{\infty} c_n^* e^{-st} dt, \quad (3.5)$$

because the transformed longitudinal moments of surface concentration $\hat{\gamma}_n^* = \mathcal{L}\{\gamma_n^*\}$ in the boundary condition can be eliminated. In Laplace space, equations (3.4) are given

by

$$\frac{\partial^2 \hat{c}_n^*}{\partial y^2} = s\hat{c}_n^* - c_n^*(t=0) - nPe u \hat{c}_{n-1}^* - n(n-1)\hat{c}_{n-2}^*, \quad (3.6a)$$

$$-\frac{\partial \hat{c}_n^*}{\partial y} = s\hat{\gamma}_n^* - \gamma_n^*(t=0) = k_a \hat{c}_n^* - k_d \hat{\gamma}_n^* \quad \text{at } y=1, \quad (3.6b)$$

$$-\frac{\partial \hat{c}_n^*}{\partial y} = 0 \quad \text{at } y=0. \quad (3.6c)$$

Since no mass is adsorbed on the wall initially, $\gamma_n^*(t=0) = 0$. A discussion of the more general initial conditions is given in appendix A. Note that the second equality in (3.6b) can be solved for $\hat{\gamma}_n^*$ as

$$\hat{\gamma}_n^* = \frac{k_a}{k_d + s} \hat{c}_n^*. \quad (3.7)$$

so that (3.6b) turns into a Robin-type boundary condition

$$-\frac{\partial \hat{c}_n^*}{\partial y} = \frac{k_a s}{k_d + s} \hat{c}_n^* \quad \text{at } y=1. \quad (3.8)$$

The δ -function initial distribution of solute leads to the following initial conditions

$$c_0^* = 1, \quad c_1^* = c_2^* = 0 \quad \text{at } t=0. \quad (3.9)$$

Therefore, equation (3.6a), together with boundary conditions (3.6c) and (3.8), gives the following system of ordinary differential equations (ODEs) for \hat{c}_0^* , \hat{c}_1^* and \hat{c}_2^* ,

$$\frac{d^2 \hat{c}_0^*}{dy^2} = s\hat{c}_0^* - 1, \quad (3.10a)$$

$$\frac{d^2 \hat{c}_1^*}{dy^2} = s\hat{c}_1^* - Pe u \hat{c}_0^*, \quad (3.10b)$$

$$\frac{d^2 \hat{c}_2^*}{dy^2} = s\hat{c}_2^* - 2Pe u \hat{c}_1^* - 2\hat{c}_0^*, \quad (3.10c)$$

with boundary conditions

$$\frac{d\hat{c}_n^*}{dy} = -\frac{k_a s}{k_d + s} \hat{c}_n^* \quad \text{at } y=1, \quad (3.11a)$$

$$\frac{d\hat{c}_n^*}{dy} = 0 \quad \text{at } y=0, \quad (3.11b)$$

for $n = 0, 1, 2$.

However, not the analytical solutions of $\hat{c}_n^*(y, s)$, but the transverse-averaged moments $\hat{m}_n(s) = \int_0^1 \hat{c}_n^* dy$, are of interest here. For instance, \hat{m}_0 has the form

$$\hat{m}_0 = \frac{1}{s} - \frac{k_a \sinh(\sqrt{s})}{\sqrt{s} (k_a s \cosh(\sqrt{s}) + \sqrt{s} \sinh(\sqrt{s}) (k_d + s))}. \quad (3.12)$$

The analytical form of \hat{m}_1 and \hat{m}_2 are complex (given in supplementary materials), but both of them and \hat{m}_0 can be written in a general form as

$$\hat{m}_n(s) = \frac{N_n(s)}{E(s)^{(n+1)}} \quad \text{for } n = 0, 1, 2, \quad (3.13)$$

where the denominator $E(s)$ is given by

$$E(s) = k_a s \cosh(\sqrt{s}) + (k_d + s) \sqrt{s} \sinh(\sqrt{s}), \quad (3.14)$$

which is a transcendental function of s and includes all the singularities of the moments. The numerators $N_n(s)$ are complex functions of s obtained by a computer algebra system (The MathWorks, Inc. 2012). The transcendental function $E(s)$ has two important properties:

(i) There are only first-order singularities in $E(s)$, and thus \hat{m}_0 , \hat{m}_1 and \hat{m}_2 only have first-, second- and third-order singularities, respectively. This helps to employ the residue theorem for the inverse Laplace transform.

(ii) All the singularities of $E(s) = 0$ fall along the negative axis, and thus substituting $s = -p^2$, where p is a real positive number, leads to a transcendental equation of p in the real space †,

$$\tan(p)(p^2 - k_d) - k_a p = 0. \quad (3.15)$$

Equation (3.15) has an infinite number of roots p_k , $k = 0, 1, \dots, \infty$. These roots p_k correspond to characteristic decay rates of the moments and the lowest order term with the smallest root, i.e. $p_0 = 0$, dominates the behavior at late times.

3.2. Inverse Laplace transform by the residue theorem

The inverse Laplace transform of the moments can be written as the Bromwich integral

$$m_n(t) = \frac{1}{2\pi i} \int_{\mathcal{C}} \hat{m}_n(s) e^{st} ds, \quad (3.16)$$

where $i = \sqrt{-1}$ and \mathcal{C} is a contour chosen so that all the singularities of $\hat{m}_n(s)$ are to the left of it. Further, if we apply the residue theorem to the above integral, we have

$$m_n(t) = \sum_{k=0}^{\infty} R_k, \quad (3.17)$$

where R_k are the residues of $\hat{m}_n e^{st}$ and can be calculated as

$$R_k = \frac{1}{(l-1)!} \lim_{s \rightarrow s_k} \frac{d^{l-1}}{ds^{l-1}} (\hat{m}_n e^{st} (s - s_k)^l). \quad (3.18)$$

where l is the order of the k^{th} singularity or pole s_k .

Since \hat{m}_0 , \hat{m}_1 and \hat{m}_2 only have first-, second- and third-order singularities respectively, we have

$$m_0(t) = \sum_{k=0}^{\infty} \lim_{s \rightarrow s_k} (s - s_k) \hat{m}_0 \exp(st) = \sum_{k=0}^{\infty} a_k \exp(-p_k^2 t), \quad (3.19a)$$

$$m_1(t) = \sum_{k=0}^{\infty} \lim_{s \rightarrow s_k} \frac{d}{ds} [(s - s_k)^2 \hat{m}_1 \exp(st)] = \sum_{k=0}^{\infty} b_k^{(1)} \exp(-p_k^2 t) + b_k^{(2)} t \exp(-p_k^2 t), \quad (3.19b)$$

$$\begin{aligned} m_2(t) &= \sum_{k=0}^{\infty} \frac{1}{2} \lim_{s \rightarrow s_k} \frac{d^2}{ds^2} [(s - s_k)^3 \hat{m}_2 \exp(st)] \\ &= \sum_{k=0}^{\infty} c_k^{(1)} \exp(-p_k^2 t) + c_k^{(2)} t \exp(-p_k^2 t) + c_k^{(3)} t^2 \exp(-p_k^2 t), \end{aligned} \quad (3.19c)$$

† $\tanh(ip) = i \tan(p)$ is used.

where

$$a_k = \lim_{s \rightarrow s_k} (s - s_k) \hat{m}_0, \quad (3.20a)$$

$$b_k^{(1)} = \lim_{s \rightarrow s_k} \frac{d}{ds} [(s - s_k)^2 \hat{m}_1], \quad (3.20b)$$

$$b_k^{(2)} = \lim_{s \rightarrow s_k} (s - s_k)^2 \hat{m}_1, \quad (3.20c)$$

$$c_k^{(1)} = \frac{1}{2} \lim_{s \rightarrow s_k} \frac{d^2}{ds^2} [(s - s_k)^3 \hat{m}_2], \quad (3.20d)$$

$$c_k^{(2)} = \lim_{s \rightarrow s_k} \frac{d}{ds} [(s - s_k)^3 \hat{m}_2], \quad (3.20e)$$

$$c_k^{(3)} = \frac{1}{2} \lim_{s \rightarrow s_k} (s - s_k)^3 \hat{m}_2. \quad (3.20f)$$

In order to remove the limit operator and give an explicit form of the coefficients in (3.20), the general form of moments in Laplace space (3.13) are substituted into (3.20). The fractional forms of \hat{m}_0 , \hat{m}_1 and \hat{m}_2 allow us to apply the L'Hospital's rule and obtain the explicit form of the coefficients,

$$a_k = \frac{N_0}{T_1}, \quad (3.21a)$$

$$b_k^{(1)} = \frac{T_1 N_1' - 2T_2 N_1}{T_1^3}, \quad (3.21b)$$

$$b_k^{(2)} = \frac{N_1}{T_1^2}, \quad (3.21c)$$

$$c_k^{(1)} = \frac{(12T_2^2 - 6T_1 T_3)N_2 - 6T_1 T_2 N_2' + T_1^2 N_2''}{2T_1^5}, \quad (3.21d)$$

$$c_k^{(2)} = \frac{T_1 N_2' - 3T_2 N_2}{T_1^4}, \quad (3.21e)$$

$$c_k^{(3)} = \frac{N_2}{2T_1^3}, \quad (3.21f)$$

where $N_n' = dN_n/ds$, $N_n'' = d^2N_n/ds^2$ at $s = s_k$ and $T_n = E^{(n)}/n!$ is the n^{th} order Taylor expansion coefficient of $E(s)$ at $s = s_k$. These coefficients can also be expressed in terms of p_k by substituting $s_k = -p_k^2$. The analytical expressions of a_k , $b_k^{(1)}$, $b_k^{(2)}$, $c_k^{(1)}$, $c_k^{(2)}$, $c_k^{(3)}$ are given in the supplementary materials.

To summarize, for a given k_a and k_d , equation (3.15) is first solved for a series of p_k , which are substituted into (3.21) to obtain the coefficients a_k , b_k and c_k . The normalized longitudinal moments M_0 , M_1 and M_2 , the transport velocity v and the dispersion coefficient D_L are then determined by definitions (3.1) and (3.2).

3.3. Reduction to previous results

In the long time limit, when the zeroth-order terms dominate, the transport velocity and dispersion coefficient are

$$v_0 = \frac{b_0^{(2)}}{a_0} = Pe \frac{k_d}{k_a + k_d} = Pe \frac{1}{k+1}, \quad (3.22a)$$

$$D_0 = \frac{1}{2} \left(\frac{c_0^{(2)}}{a_0} - \frac{2b_0^{(1)}b_0^{(2)}}{a_0^2} \right) = \frac{1}{1+k} + Pe^2 \frac{2}{105} \frac{1+9k+25.5k^2}{(1+k)^3} + \frac{Pe^2}{k_d} \frac{k}{(1+k)^3}, \quad (3.22b)$$

which are consistent with the results obtained in chromatography (Khan 1962). For $k > 0$, the transport velocity of the solute is slower than the mean flow velocity at late times.

At early but finite time, the first-order terms dominate and lead to an asymptotic velocity v_1 and dispersion coefficient D_1 given as

$$v_1 = \frac{b_1^{(2)}}{a_1} \quad \text{and} \quad D_1 = \frac{1}{2} \left(\frac{c_1^{(2)}}{a_1} - \frac{2b_1^{(1)}b_1^{(2)}}{a_1^2} \right). \quad (3.23a,b)$$

In the limiting case of $k_d = 0$ analysed by Lungu & Moffatt (1982), the zeroth-order coefficients of the moments vanish, i.e. $a_0 = b_0^{(2)} = b_0^{(1)} = c_0^{(3)} = c_0^{(2)} = c_0^{(1)} = 0$. Therefore, the first-order terms dominate and lead to the following asymptotic transport velocity and dispersion coefficient,†

$$v_{LM} = \frac{Pe (4k_a^2 p_1^2 + 3k_a^2 + 3k_a + 4p_1^4 - 3p_1^2)}{4p_1^2 (k_a^2 + k_a + p_1^2)}, \quad (3.24a)$$

$$\begin{aligned} D_{LM} = 1 + & \left(Pe^2 (-8k_a^6 p_1^4 + 150k_a^6 p_1^2 - 315k_a^6 - 56k_a^5 p_1^4 + 750k_a^5 p_1^2 \right. \\ & - 945k_a^5 - 24k_a^4 p_1^6 + 282k_a^4 p_1^4 + 555k_a^4 p_1^2 - 945k_a^4 - 192k_a^3 p_1^6 \\ & + 1560k_a^3 p_1^4 - 540k_a^3 p_1^2 - 315k_a^3 - 24k_a^2 p_1^8 - 78k_a^2 p_1^6 + 1455k_a^2 p_1^4 \\ & \left. - 495k_a^2 p_1^2 - 136k_a p_1^8 + 810k_a p_1^6 + 225k_a p_1^4 - 8p_1^{10} - 210p_1^8 + 585p_1^6) \right) \\ & / \left(160p_1^6 (k_a^2 + k_a + p_1^2)^3 \right), \quad (3.24b) \end{aligned}$$

where p_1 is determined by solving (3.15). Equations (3.24) are consistent with (3.4) and (3.11) given in Lungu & Moffatt (1982), except for a difference in notation. For $k_a > 0$, the asymptotic transport velocity of the solute is faster than the mean flow velocity. Note that the early and late transport velocity v_1, v_0 have linear dependence on Pe and the early and late dispersion coefficient D_1, D_0 (excluding contribution from pure diffusion) have quadratic dependence on Pe so that the normalized ones defined in (4.1) below are generally independent of Pe .

3.4. Equilibrium sorption model

If the kinetics of the reactions are fast enough that local chemical equilibrium is valid, the linear kinetic sorption model reduces to the linear isotherm (i.e., equilibrium sorption model) $\gamma = kc$, with $k = k_a/k_d$. For the equilibrium sorption model, equation (3.15) becomes

$$\tan(p) = -kp, \quad (3.25)$$

† There is a typo in D_{LM} in published version. Here it has been corrected.

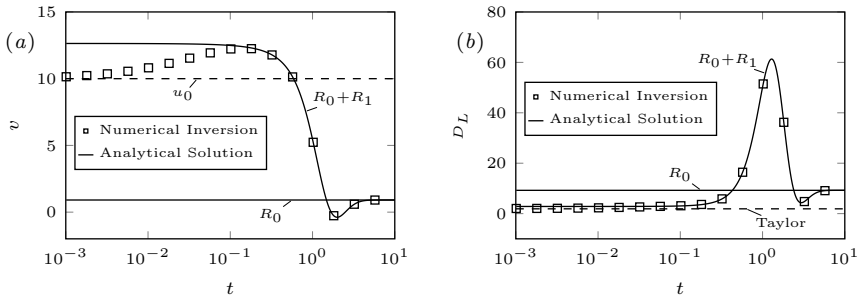


FIGURE 2. Comparison of the zeroth-order approximation (R_0) and the first-order approximation ($R_0 + R_1$) with the numerical inversion of the Laplace transform (squares) using Talbot’s method. R_0 and R_1 are the zeroth and first residues of the moments defined in equation (3.17) and (3.18). Results are shown for $Pe = 10$, $k_a = 10$, $k_d = 1$. Panel (a) shows the transport velocity v , where the mean flow velocity $u_0 = U_0 H/D = Pe$. Panel (b) shows the dispersion coefficient D_L , where the dashed line labelled as Taylor denotes the Taylor dispersion $2/105Pe^2$.

which can be solved for a series of p_k . Taking the limit $k_a \rightarrow \infty$, $k_d \rightarrow \infty$ of (3.21) while keeping $k_a/k_d = k$, the coefficients become only functions of the partition coefficient k , as expected.

3.5. First-order approximation of the series solution

For the general case when k_d is not zero, the fast transport described by (3.24) may survive at early times before desorption has come into play. In this case, the general series solution of the moments (3.19) allows us to study the transition from fast transport at early times described by first-order terms to slow transport at late times described by zeroth-order terms.

The zeroth- and first-order terms corresponds to the residues R_0 and R_1 in (3.17). Figure 2(a) and 2(b) show the comparison of the zeroth-order approximation R_0 and first-order approximation $R_0 + R_1$ with the numerical inversion of Laplace transform using Talbot’s method (Abate & Whitt 2006; McClure 2013). As expected, the first-order approximation $R_0 + R_1$ captures the solution at both the early and the late times, while the zeroth-order approximation R_0 only describes the late time behavior. Additional tests show that the first-order approximation is sufficient to describe the solution for a large range of k_a and k_d after a short initial time. Therefore, we truncate the series solution (3.19) by retaining only the zeroth- and first-order terms,

$$m_0 = a_0 + a_1 \exp(-p_1^2 t), \quad (3.26a)$$

$$m_1 = (b_0^{(1)} + b_0^{(2)} t) + (b_1^{(1)} + b_1^{(2)} t) \exp(-p_1^2 t), \quad (3.26b)$$

$$m_2 = (c_0^{(1)} + c_0^{(2)} t + c_0^{(3)} t^2) + (c_1^{(1)} + c_1^{(2)} t + c_1^{(3)} t^2) \exp(-p_1^2 t), \quad (3.26c)$$

where the higher-order terms describing the very early time behavior are ignored.

4. Regimes of transport

In this section, we discuss the transition from the early fast transport to the late slow transport. Numerical simulations of the full two-dimensional problem illustrate the physical mechanism that leads to this transition. The truncated analytical solution provides the estimates of the associated time scales. First, we will use the simpler

equilibrium sorption model to discuss the regime transition, followed by the more general kinetic case.

4.1. Two-dimensional simulations

Figure 3 shows two-dimensional simulations of the solute concentration at different times for $Pe = 10$, $k_a = 50$ and $k_d = 1$. The full problem is numerically solved by the Lattice Boltzmann Method (LBM) (Chen & Doolen 1998; Wang & Kang 2010; Zhang & Wang 2015). The δ -function initial condition is approximated by a piecewise constant function that is non-zero in a small interval around the origin. This approximation of the initial condition only affects the results in a short diffusive transient and the results agree well with the analytical solution (figure 3*f-3h*).

Initially, the strong adsorption removes the solute from the slow-moving fluid near the wall. The remaining solute in the center of the channel forms a fast-moving pulse (figure 3*b* and 3*c*), particularly evident in the transversely-averaged concentration shown in figure 3(*e*). This corresponds to the increased solute transport velocity in the irreversible sorption case (Lungu & Moffatt 1982). This regime persists as long as adsorption dominates.

However, the fast-moving pulse decays rapidly and eventually desorption releases solute in its wake (figure 3*d*). As the amount of desorbed solute in the slow-moving fluid near the wall increases, the solute transport velocity declines. This process continues until desorption at the back balances adsorption at the front. The transport velocity and dispersion coefficient will approach the slow transport described by the one-dimensional model of the transversely-averaged concentration in the reversible sorption case (Khan 1962).

4.2. Equilibrium sorption model

Following the solution procedure in section 3.4, this section presents results and analysis for equilibrium sorption model, $\gamma = kc$. To demonstrate the different transport behaviors, we define a normalized transport velocity \mathcal{V} and a normalized dispersion coefficient \mathcal{D} as

$$\mathcal{V} = \frac{v}{Pe} \quad \text{and} \quad \mathcal{D} = \frac{D_L - 1}{D_t}, \quad (4.1a,b)$$

where $D_t = 2/105Pe^2$ is the Taylor dispersion coefficient for a tracer in Poiseuille flow and the unit contribution of diffusion has been subtracted in the numerator of (4.1*b*). In this way, $\mathcal{V} > 1$ ($\mathcal{D} > 1$) means increased velocity (dispersion) relative to a nonreactive tracer while $\mathcal{V} < 1$ ($\mathcal{D} < 1$) means decreased velocity (dispersion).

Figure 4 shows the evolution of the position of the center of mass M_1 and the normalized transport velocity \mathcal{V} for different partition coefficients. For $k > 10$, a linear region emerges at early times in figure 4(*a*), corresponding to an initial plateau in figure 4(*b*). This corresponds to the well-developed early regime characterized by fast transport, approaching an asymptotic velocity $1 + 3/\pi^2 \approx 1.3$. This is consistent with the results in an adsorption-only case with $k_a \rightarrow \infty$ (Lungu & Moffatt 1982). After a transition period, a second linear region at late times appears, corresponding to the decreased transport velocity $1/(1+k)$.

Figure 5 shows similar behaviors of the variance of solute mass in the fluid M_2 and the normalized dispersion coefficient \mathcal{D} . In the early regime, the dispersion coefficient is reduced relative to a tracer with $\mathcal{D} \sim 0.14$, which also agrees with the adsorption-only case with $k_a \rightarrow \infty$. In the late regime, the dispersion coefficient is given by the first two terms of (3.22*b*), first obtained by Golay (1958).

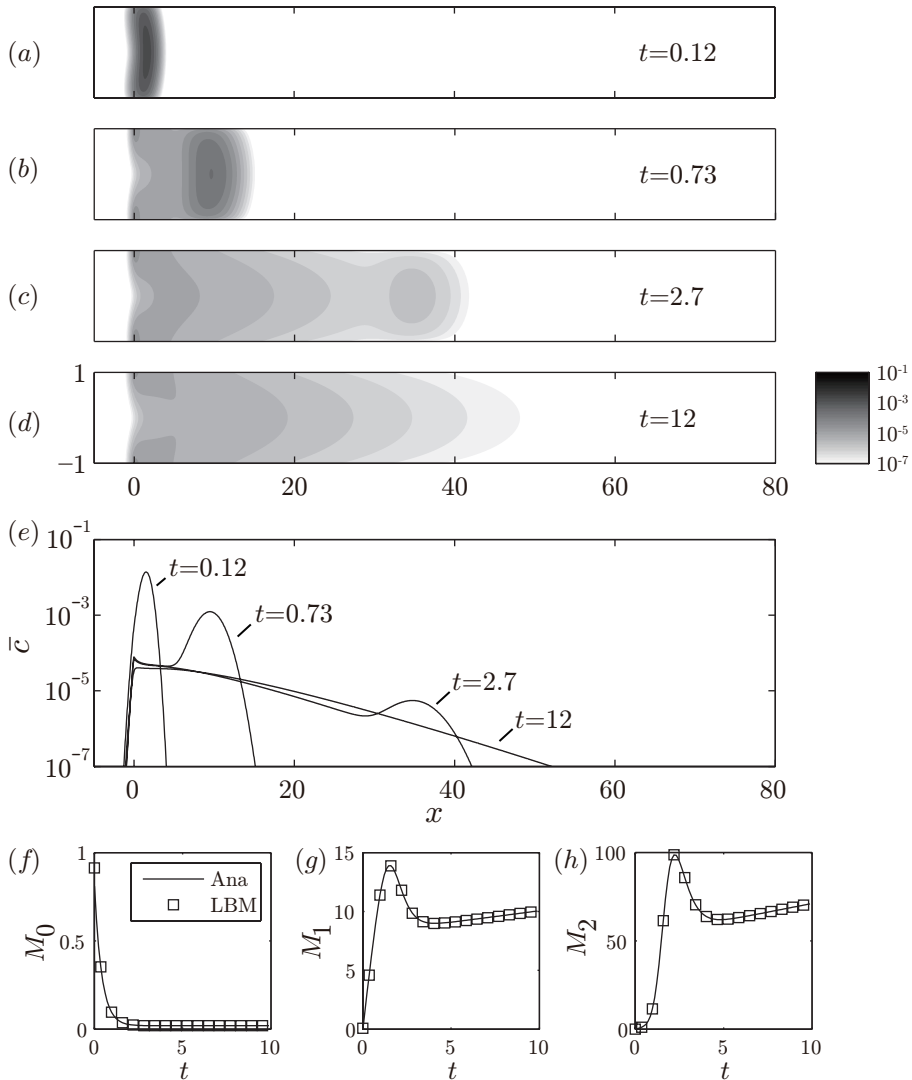


FIGURE 3. Two dimensional simulation of solute transport with sorption in Poiseuille flow with $Pe = 10$, $k_a = 50$ and $k_d = 1$. Panel (a–d) show concentration distribution and panel (e) shows transversely-averaged concentration profile at $t = 0.12, 0.73, 2.7, 12$. Panel (f–h) show the evolution of the zeroth-, first- and second-order moments and compare the numerical simulation (LBM) with the first-order approximation of the analytical solution (Ana).

Between the early and late time, there is a drastic transition of the transport behavior. Especially when k is large, both M_1 and M_2 decrease after reaching maxima during the transition and this leads to negative velocity and dispersion coefficient. Physically, it means that desorption near the origin dominates over the fast-moving pulse in figure 3 so that the center of mass shifts backwards and the variance reduces because the transversely-averaged concentration distribution changes from a bimodal type (one peak near the origin and the other at the pulse front) to a unimodal type (single peak near the origin).

To compare the early and late behaviors as a function of k , we define the normalized

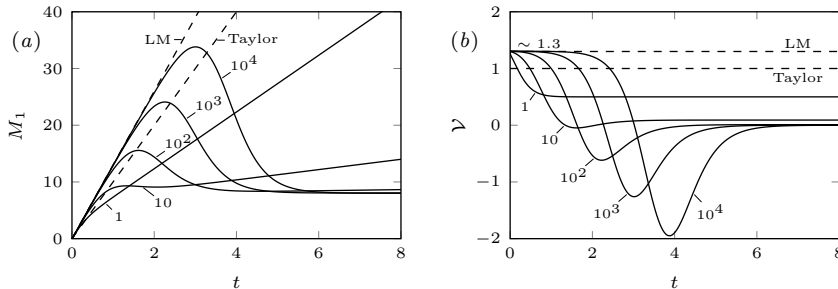


FIGURE 4. Evolution of (a) center of mass M_1 and (b) normalized transport velocity \mathcal{V} for different partition coefficients k . Dashed lines with labels LM and Taylor stand for the asymptotic regime of an adsorption-only case (Lungu & Moffatt 1982) and the asymptotic regime of a nonreactive tracer, respectively.

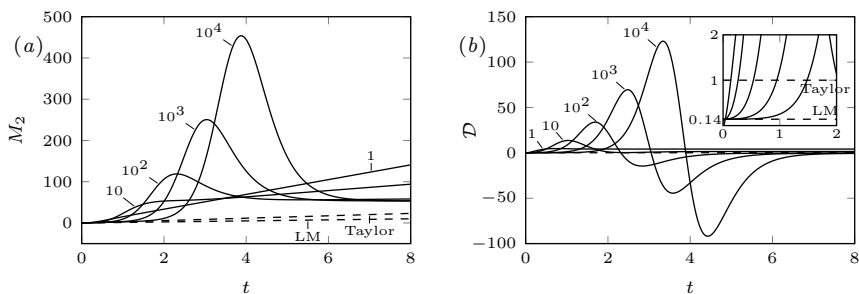


FIGURE 5. Evolution of (a) variance of solute mass distribution M_2 and (b) the normalized dispersion coefficient \mathcal{D} for different partition coefficients k . Dashed lines with labels LM and Taylor stand for the asymptotic regime of an adsorption-only case (Lungu & Moffatt 1982) and the asymptotic regime of a nonreactive tracer, respectively.

early and late velocities as

$$\mathcal{V}_e = \frac{v_1}{Pe} \quad \text{and} \quad \mathcal{V}_l = \frac{v_0}{Pe}, \quad (4.2a,b)$$

and similarly we define normalized early and late dispersion coefficients as

$$\mathcal{D}_e = \frac{D_1 - 1}{D_t} \quad \text{and} \quad \mathcal{D}_l = \frac{D_0 - 1/(1+k)}{D_t}, \quad (4.2c,d)$$

where v_0 , D_0 and v_1 , D_1 are obtained from the zeroth- and first-order terms of the solution, the equilibrium limits of (3.22) and (3.23). Note that at early times the effective diffusion is not affected by sorption while it is reduced by a factor of $1/(1+k)$ at late times.

As shown in figure 6, for large k the difference of normalized transport velocity between \mathcal{V}_e and \mathcal{V}_l is the largest and the normalized early-time dispersion coefficient \mathcal{D}_e asymptotes to 0.14. The normalized late-time dispersion coefficient \mathcal{D}_l first increases with k , then reduces towards 0. For small k , the early velocity \mathcal{V}_e and dispersion coefficient \mathcal{D}_e don't reach the asymptotic values 1.3 and 0.14. In this case, the early regime is not well-developed and the first-order terms of the solution are not dominant. Therefore, \mathcal{V}_e and \mathcal{D}_e don't represent the transport behavior in this case.

For a tracer in Poiseuille flow, the preasymptotic transport before equilibrium has been studied extensively (e.g. Gill & Sankarasubramanian 1970; Haber & Mauri 1988;

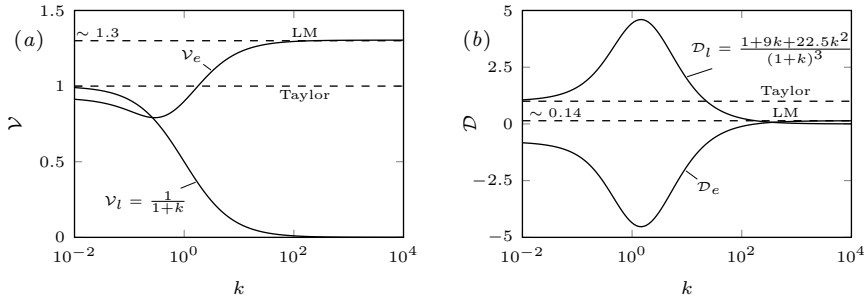


FIGURE 6. (a) Normalized early velocity $\mathcal{V}_e = v_1/Pe$, late velocity $\mathcal{V}_l = v_0/Pe$ and (b) normalized early dispersion coefficient $\mathcal{D}_e = (D_1 - 1)/D_t$, late dispersion coefficient $\mathcal{D}_l = (D_0 - 1/(1+k))/D_t$ as a function of partition coefficient k .

Mercer & Roberts 1990; Latini & Bernoff 2001; Dentz & Carrera 2007; Bolster *et al.* 2011; Wang *et al.* 2012). Typically, diffusion dominates when $t \ll t_d = Pe^{-2/3}$ and after the characteristic equilibrium time scale, $t = 1$, solute transport can be described by the transversely-averaged model with the mean flow velocity and the dispersion coefficient D_t . However, for a reactive case considered here, the time scale to reach equilibrium can be quite different from the tracer case because surface reactions introduce additional characteristic time scales.

In the first-order approximation (3.26), a series of time scales can be defined by comparing the zeroth-order and first-order terms. Take m_0 as an example, by comparing a_0 and $a_1 \exp(-p_1^2 t)$, we can define a time scale as

$$t_1 = \frac{1}{p_1^2} \ln \frac{a_1}{a_0} = \frac{1}{p_1^2} \ln \frac{2k^2(k+1)}{k^2 p_1^2 + k + 1}. \quad (4.3)$$

This time scale indicates the transition from the early regime when the transport is dominated by the first-order terms to the late regime dominated by the zeroth-order terms. Similarly, other time scales can be determined by comparing b_k and c_k . We notice that the coefficients in the series solution have the following property

$$\frac{a_1}{a_0} < \frac{b_1^{(2)}}{b_0^{(2)}} \sim \frac{c_1^{(2)}}{c_0^{(2)}} < \frac{c_1^{(3)}}{c_0^{(3)}}, \quad (4.4)$$

which means that t_1 will give the smallest time scale. At the same time, since the time scales for the velocity determined by $b_1^{(2)}/b_0^{(2)}$ and the dispersion coefficient determined by $c_1^{(2)}/c_0^{(2)}$ have the same scaling, we can choose

$$t_2 = \frac{1}{p_1^2} \ln \frac{b_1^{(2)}}{b_0^{(2)}} = \frac{1}{p_1^2} \ln \frac{k^2(k+1)^2(4k^2 p_1^4 + 3k^2 p_1^2 - 3k + 4p_1^2 - 3)}{2p_1^2(k^2 p_1^2 + k + 1)^2} \quad (4.5)$$

as a critical time scale, after which the zeroth-order terms dominate and the late time behavior emerges. Note that both of the time scales are not dependent on Pe . Consequently, the transient solute transport with sorption can be divided into the following three regimes,

- (I) $0 < t < t_1$: early regime with fast transport
- (II) $t_1 < t < t_2$: transition period
- (III) $t_2 < t$: late regime with slow transport

As shown in figure 4 and 5, the duration of the early regime, as well as the transition

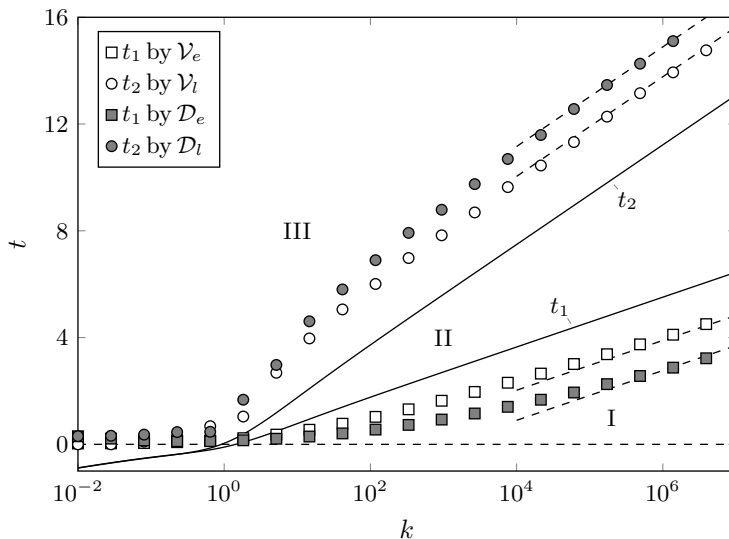


FIGURE 7. Variation of the early time scale t_1 and the late time scale t_2 as functions of different partition coefficient k . The solid lines show t_1 and t_2 from (4.3) and (4.5), respectively and the dashed lines indicate the scalings for large k given by (4.6), which have been shifted to match the symbols determined by the numerical inverse Laplace transform. White symbols are determined by velocity and gray symbols are determined by dispersion coefficient. The transient solute transport with sorption is divided into three regimes: (I) early regime with fast transport; (II) transition period; (III) late regime with slow transport.

period, increases with increasing k . In the limit of large k , we have

$$\lim_{k \rightarrow \infty} t_1 = \frac{4}{\pi^2} \ln k \quad \text{and} \quad \lim_{k \rightarrow \infty} t_2 = \frac{8}{\pi^2} \ln k, \quad (4.6a,b)$$

where we have used $\lim_{k \rightarrow \infty} p_1 = \pi/2$. Equations (4.6) predict a linear relationship between t_1 , t_2 and $\ln k$ when k is large and $t_2 \sim 2t_1$. Figure 7 compares results from the numerical inverse Laplace transform with these analytically determined time scales as a function of k . When $k \gg 1$, t scales with $\ln k$, as predicted by (4.6). For small k , the early regime is so short that it is generally not observed.

4.3. Kinetic sorption model

In the kinetic sorption model, there are two additional governing parameters, namely, the dimensionless adsorption rate constant k_a and the dimensionless desorption rate constant k_d . Generally, a similar transition from early to late behavior can be observed and the equilibrium results are recovered when kinetics are fast, i.e. $k_a \gg 1$ and $k_d \gg 1$.

Similar to the way that the time scales are determined for the equilibrium model, we can obtain t_1 and t_2 for the kinetic model using (4.3) and (4.5),

$$t_1 = \frac{1}{p_1^2} \ln \frac{2k_a^2(k_a + k_d)}{k_d(p_1^4 + (k_a^2 + k_a - 2k_d)p_1^2 + k_a k_d + k_d^2)}, \quad (4.7a)$$

$$t_2 = \frac{1}{p_1^2} \ln \frac{k_a^2(k_a + k_d)^2(4p_1^6 + (4k_a^2 - 8k_d - 3)p_1^4 + (3k_a^2 + 3k_a + 4k_d^2 + 6k_d)p_1^2 - 3k_a k_d - 3k_d^2)}{2k_d^2 p_1^2 (p_1^4 + (k_a^2 + k_a - 2k_d)p_1^2 + k_a k_d + k_d^2)^2}, \quad (4.7b)$$

which are shown in figure 8.

The early regime is only observed when k_a exceeds k_d . In all other cases, transition occurs from the very beginning followed by a dominated late regime. When both k_a and k_d are large, the time scales of the kinetic model recover those of the equilibrium model.

However, if the rates decrease, the kinetic time scales become longer. In this case, the root p_1 of (3.15) can be approximated by $p_1^2 \approx k_a + k_d$ using Taylor expansion for $\tan(p)$. Then the ratios a_1/a_0 and $b_1^{(2)}/b_0^{(2)}$ used to obtain the time scales simplify to

$$\frac{a_1}{a_0} = \frac{2k_a}{k_d(k_a + 2)} \quad \text{and} \quad \frac{b_1^{(2)}}{b_0^{(2)}} = \frac{k_a^2(4k_a + 4k_d + 7)}{2k_d^2(k_a + 2)^2}. \quad (4.8a,b)$$

This analysis shows that both time scales increase dramatically in the lower left region where k_a and k_d are small in figure 8. In this region, the duration of the early regime is long, but the deviations of velocity and dispersion coefficient from the tracer case are minor as the limiting values given by the adsorption-only case approach unity with small k_a . Physically, this region corresponds to a kinetically slow-sorbing ($k_a, k_d \ll 1$) solute with a large partition coefficient $k \gg 1$.

The analytical solution presented in §3.3 recovers the previous analysis in the limit of $k_d = 0$ (Lungu & Moffatt 1982). This limiting solution puts an upper bound on the transport velocity and a lower bound on the dispersion coefficient in the early regime. If the early regime is well-developed, the limiting solution given by Lungu & Moffatt (1982) provides a good approximation for finite k_d , see figure 8(c). The well-developed early regime is indicated by gray shadings in figure 8(a), where the early-time asymptotic transport velocity and dispersion coefficient given by (3.23) are within 10% of the limiting values given by Lungu & Moffatt (1982). Case A, B, C give examples of well-developed early regime, while the velocity doesn't reach the asymptotic value in case D. Generally, if $k > 10$ (> 1000), the early-time velocity (dispersion coefficient) are well developed. Note that the first-order analytical solution for transport velocity ($R_0 + R_1$) shown in figure 8(c) is computed by (3.2) and (3.26).

5. Conclusion

In this work, we reconcile two different analyses of solute transport with sorption in Poiseuille flow that reached apparently contradictory conclusions. We show that these two analyses capture different regimes of the transport. Generally, the solute experiences an early regime with fast transport velocity if adsorption dominates desorption. At late times, when desorption becomes important, the solute transport slows down. This leads to a regime transition that scales as $\ln k$ for the equilibrium sorption model, where k is the dimensionless partition coefficient. Therefore, the early regime is more pronounced when k is large. In the kinetic sorption model, the early regime is also observed if the kinetics are slow and the dimensionless adsorption rate constant k_a exceeds the dimensionless desorption rate constant k_d . As long as $k_a \gg k_d$, the early regime is well-developed and the transport velocity and the dispersion coefficient in this early regime are well approximated by the analysis of Lungu & Moffatt (1982) in the limit of $k_d = 0$.

The time scales presented in this work allow the determination of the dominant transport behavior for a given application. Experience shows that the late regime dominates the subsurface transport of sorbing contaminants in fractures. However, the early regime may be important in the biomedical applications where transport occurs over smaller distances. Our analysis may also allow a design of chromatography columns that can achieve opposite separation results.

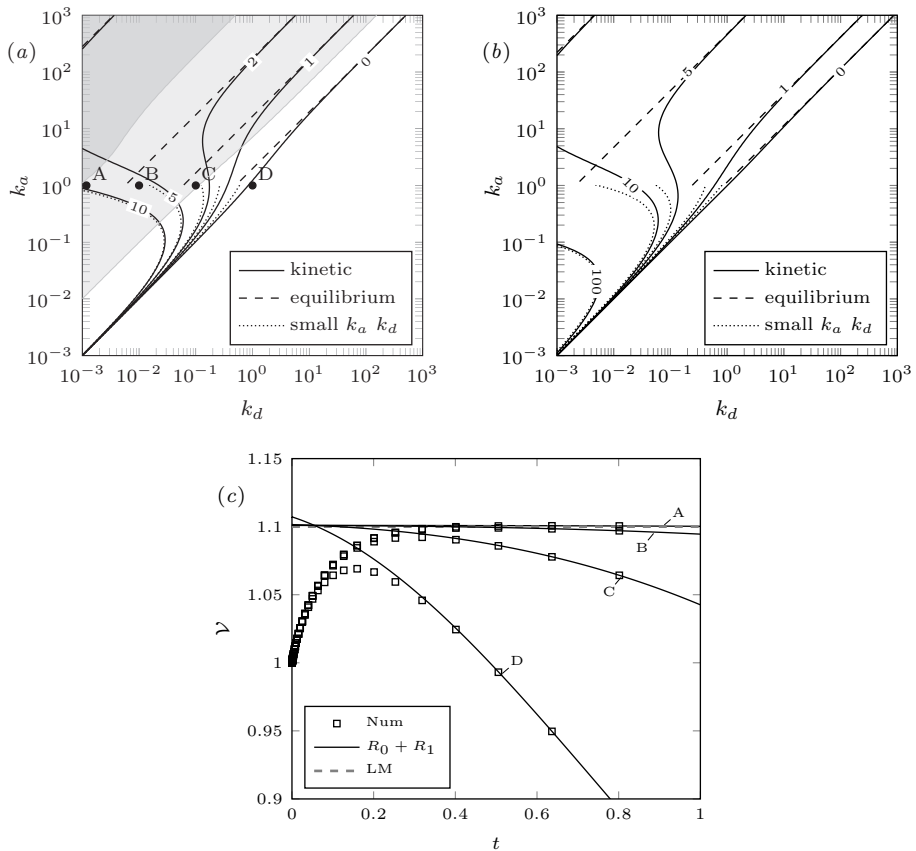


FIGURE 8. Contour lines of (a) the early time scale t_1 and (b) the late time scale t_2 for the kinetic sorption model. Dashed lines represent the time scales obtained from the equilibrium sorption model for large k_a and k_d and dotted lines represent approximations for small k_a and k_d , given by (4.8). Shaded area in (a) represents the region where the early regime is well-developed, i.e., the velocity (light-shaded area) and dispersion coefficient (dark-shaded area) are close to the limiting values given by the adsorption-only case. Panel(c) shows the evolution of velocity at early time for the conditions labeled as A, B, C, D in panel(a). Symbols are the results from full numerical inverse Laplace transform, solid lines are first-order approximation of the analytical solution and dashed line is the asymptotic value for $k_d = 0$ at $k_a = 1$, given by Lungu & Moffatt (1982).

L. Zhang and M. Hesse are grateful to Prof. Howard Stone and Dr. Zhong Zheng for helpful discussions, which motivate this work. The authors are also grateful to Prof. Howard Stone for carefully reading the manuscript. L. Zhang acknowledges the financial support by China Scholarship Council's (CSC) Chinese Government Graduate Student Oversea Study Program. M. Wang acknowledges the financial support by the NSF grant of China (No.51676107, 91634107, U1562217), National Science and Technology Major Project on Oil and Gas (No.2017ZX05013001).

Appendix A. Effect of initial condition

The initial distribution of solute mass manifest itself either as a source term, $c_n^*(t = 0)$, or a constant in the boundary condition, $\gamma_n^*(t = 0)$, in the ODE system (3.10). These

effects can be important in our problem in the sense that it may affect the form of the solutions of the moments. General discussion on this topic is out of the scope of this paper, and we show a special case as an example.

In the previous formulation, we assume initially there is no mass adsorbed on the wall, $\gamma_n^*(t=0) = 0$. In this section, we change the initial condition by retaining the uniform release in the fluid, but assuming the mass distribution between the wall and the bulk has reached equilibrium, namely, $c(t=0) = \delta(x)/(1+k)$, $\gamma(t=0) = \delta(x)k/(1+k)$. Following the same procedure in §3.1 and §3.2, we find that the moments in Laplace space $\hat{m}_0, \hat{m}_1, \hat{m}_2$ are no longer in the form of (3.13), but with a slight difference,

$$\hat{m}_0(s) = \frac{Q_0(s)}{s}, \quad (\text{A } 1a)$$

$$\hat{m}_1(s) = \frac{Q_1(s)}{sE(s)}, \quad (\text{A } 1b)$$

$$\hat{m}_2(s) = \frac{Q_2(s)}{sE^2(s)}, \quad (\text{A } 1c)$$

where Q_0, Q_1 and Q_2 are different from N_0, N_1 and N_2 . In fact, $Q_0 = 1/(1+k)$. Essentially, the order of the all the singularities, other than the zeroth-order, reduce one in the solutions. Therefore, the series solutions obtained by residue theorem are written as

$$m_0(t) = a_0, \quad (\text{A } 2a)$$

$$m_1(t) = b_0^{(1)} + b_0^{(2)}t + \sum_{k=1}^{\infty} \tilde{b}_k^{(1)} \exp(-p_k^2 t) \quad (\text{A } 2b)$$

$$m_2(t) = c_0^{(1)} + c_0^{(2)}t + c_0^{(3)}t^2 + \sum_{k=0}^{\infty} \tilde{c}_k^{(1)} \exp(-p_k^2 t) + \tilde{c}_k^{(2)}t \exp(-p_k^2 t). \quad (\text{A } 2c)$$

where $\tilde{b}_k^{(1)}, \tilde{c}_k^{(1)}$ and $\tilde{c}_k^{(2)}$ are different from $b_k^{(1)}, c_k^{(1)}$ and $c_k^{(2)}$. Note that the long-time velocity and dispersion coefficient determined by $a_0, b_0^{(2)}, c_0^{(2)}$ don't change. However, since $b_k^{(2)}$ diminishes, the early regime will not be well-developed in this case. Physically, the solute that is initially adsorbed onto the wall begins to desorb much earlier, and hence reduces the duration of the early regime. In the limit of $k_d = 0, k \rightarrow \infty$ and the initial solute mass in the fluid $c(t=0)$ vanishes so that the results by Lungu & Moffatt (1982) can not be properly recovered in this case.

REFERENCES

- ABATE, J. & WHITT, W. 2006 A unified framework for numerically inverting Laplace transforms. *INFORMS J. Comput.* **18** (4), 408–421.
- ARIS, R. 1956 On the dispersion of a solute in a fluid flowing through a tube. *Proc. R. Soc. Lond. A* **235** (1200), 67–77.
- BALAKOTIAH, V. & CHANG, H. C. 1995 Dispersion of chemical solutes in chromatographs and reactors. *Phil. Trans. R. Soc. Lond. A* **351** (1695), 39–75.
- BARTON, N. G. 1984 An asymptotic theory for dispersion of reactive contaminants in parallel flow. *J. Aust. Math. Soc. B* **25**, 287–310.
- BISWAS, R. R. & SEN, P. N. 2007 Taylor dispersion with absorbing boundaries: a stochastic approach. *Phys. Rev. Lett.* **98** (16), 164501.
- BOLSTER, D., VALDÉS-PARADA, F. J., LEBORGNE, T., DENTZ, M. & CARRERA, J. 2011 Mixing in confined stratified aquifers. *J. Contam. Hydrol.* **120**, 198–212.

- CHEN, S. & DOOLEN, G.D. 1998 Lattice Boltzmann method for fluid flows. *Annu. Rev. Fluid Mech.* **30** (1), 329–364.
- DE GANCE, A. E. & JOHNS, L. E. 1978*a* On the dispersion coefficients for Poiseuille flow in a circular cylinder. *Appl. Sci. Res.* **34** (2-3), 227–258.
- DE GANCE, A. E. & JOHNS, L. E. 1978*b* The theory of dispersion of chemically active solutes in a rectilinear flow field. *Appl. Sci. Res.* **34** (2-3), 189–225.
- DENTZ, M. & CARRERA, J. 2007 Mixing and spreading in stratified flow. *Phys. Fluids* **19** (1).
- GILL, W. N. & SANKARASUBRAMANIAN, R. 1970 Exact analysis of unsteady convective diffusion. *Proc. R. Soc. Lond. A* **316** (1526), 341–350.
- GOLAY, M. J. E. 1958 Theory of chromatography in open and coated tubular columns with round and rectangular cross-sections. In *Gas Chromatography* (ed. D. H. Desty), pp. 36–53. Butterworths.
- HABER, S. & MAURI, R. 1988 Lagrangian approach to time-dependent laminar dispersion in rectangular conduits. part 1. two-dimensional flows. *J. Fluid Mech.* **190**, 201–215.
- HESSE, F., HARMS, H., ATTINGER, S. & THULLNER, M. 2010 Linear exchange model for the description of mass transfer limited bioavailability at the pore scale. *Environ. Sci. Technol.* **44** (6), 2064–71.
- HLUSHKOU, D., GRITTI, F., GUIOCHON, G., SEIDEL-MORGENSTERN, A. & TALLAREK, U. 2014 Effect of adsorption on solute dispersion: a microscopic stochastic approach. *Anal. Chem.* **86** (9), 4463–70.
- KHAN, M. K. 1962 Non-equilibrium theory of capillary columns and the effect of interfacial resistance on column efficiency. In *Gas Chromatography* (ed. M. Van Swaay), pp. 3–17. Butterworths.
- LATINI, M & BERNOFF, A. J. 2001 Transient anomalous diffusion in Poiseuille flow. *J. Fluid Mech.* **441**, 399–411.
- LUNGU, E. M. & MOFFATT, H. K. 1982 The effect of wall conductance on heat diffusion in duct flow. *J. Engng Math.* **16** (2), 121–136.
- MCCLURE, T. 2013 Numerical inverse Laplace transform. Computer software. Mathworks File Exchange, Web. 1 Mar. 2016.
- MERCER, G. N. & ROBERTS, A. J. 1990 A centre manifold description of contaminant dispersion in channels with varying flow properties. *SIAM J. Appl. Math.* **50** (6), 1547–1565.
- MIKELIĆ, ANDRO, DEVIGNE, VINCENT & VAN DUIJN, C. J. 2006 Rigorous upscaling of the reactive flow through a pore, under dominant Peclet and Damkohler numbers. *SIAM J. Math. Anal.* **38** (4), 1262–1287.
- PAINÉ, M. A., CARBONELL, R. G. & WHITAKER, S. 1983 Dispersion in pulsed systems – I: Heterogenous reaction and reversible adsorption in capillary tubes. *Chem. Eng. Sci.* **38** (11), 1781–1793.
- SANKARASUBRAMANIAN, R. & GILL, W. N. 1973 Unsteady convective diffusion with interphase mass transfer. *Proc. R. Soc. Lond. A* **333** (1592), 115–132.
- SHAPIRO, M. & BRENNER, H. 1986 Taylor dispersion of chemically reactive species: irreversible first-order reactions in bulk and on boundaries. *Chem. Eng. Sci.* **41** (6), 1417–1433.
- SHIPLEY, R. J. & WATERS, S. L. 2012 Fluid and mass transport modelling to drive the design of cell-packed hollow fibre bioreactors for tissue engineering applications. *Math. Med. Biol.* **29** (4), 329–59.
- SMITH, R. 1983 Effect of boundary absorption upon longitudinal dispersion in shear flows. *J. Fluid Mech.* **134**, 161–177.
- TAYLOR, G. I. 1953 Dispersion of soluble matter in solvent flowing slowly through a tube. *Proc. R. Soc. Lond. A* **219** (1137), 186–203.
- THE MATHWORKS, INC. 2012 *MATLAB and Symbolic Toolbox Release 2012b*. Natick, Massachusetts, United States.
- WANG, L., CARDENAS, M. B., DENG, W. & BENNETT, P. C. 2012 Theory for dynamic longitudinal dispersion in fractures and rivers with Poiseuille flow. *Geophys. Res. Lett.* **39** (5), 105401.
- WANG, M. & KANG, Q. 2010 Modeling electrokinetic flows in microchannels using coupled lattice Boltzmann methods. *J. Comput. Phys.* **229** (3), 728–744.
- WELS, C., SMITH, L. & BECKIE, R. 1997 The influence of surface sorption on dispersion in parallel plate fractures. *J. Contam. Hydrol.* **28** (1-2), 95–114.

ZHANG, L. & WANG, M. 2015 Modeling of electrokinetic reactive transport in micropore using a coupled lattice Boltzmann method. *J. Geophys. Res.* **120** (5), 2877–2890.